Military Technical College,
Kobry El-Kobbah,
Cairo, Egypt

9th International Conference
On Aerospace Sciences &
Aviation Technology

Drag Reduction of a Circular Cylinder with Fluid Slip

Keizo Watanabe* and Takao Fujita**

ABSTRACT

Experiments were carried out on the flow visualization and velocity measurement of the wake behind a circular cylinder with a highly water-repellent wall with many fine grooves at the surface, in the Reynolds number range of Re=20～150. By applying the boundary condition of fluid slip at the wall, the streamlines of flow past a circular cylinder were analyzed at Re=20 and 50 using the numerical calculation model. The analytical results were in good quantitative agreement with the experimental trace of the flow pattern, and the drag reduction phenomena of a circular cylinder were clarified from the calculated results of the pressure profile and the experimental result of the velocity profile of the wake. The drag reduction ratios of tap water, calculated using β=4 pa·s/m for the sliding coefficient, are 15% and 10% at Re=20 and 50, respectively.

KEY WORDS

Circular Cylinder, Flow Visualization, Highly Water-Repellent Wall, Fluid Slip, Drag Reduction

* Professor, Department of Mechanical Engineering, Tokyo Metropolitan University, Tokyo, Japan.

** System Engineer of NTT Data Co. Ltd.

1. INTRODUCTION

Flow past a circular cylinder is one of the most simple and important flows around a bluff body, which is related to a column used in construction in the sea. Thus, the flow characteristics have been experimentally and theoretically studied by many researchers, and it is well known that the variation of the drag coefficient with the Reynolds number can be expressed by a single curve in Newtonian fluids [1-5]. Total drag of a circular cylinder is given as the sum of viscous drag and pressure drag. Viscous drag gives a minor contribution, with the exception of in the low Reynolds number range. The decrease of pressure drag necessitates a change of the flow pattern around a circular cylinder. Since the Toms' effect [6] was reported, in which the friction factor of polymer solutions in a circular pipe is reduced compared with that of solvent solutions in the turbulent flow range, many studies on drag reduction phenomena have been carried out from the viewpoint of energy saving [7]. However, it is very difficult to reduce the drag of Newtonian fluids in the laminar flow region, and there are very few studies on laminar drag reduction of flow around a circular cylinder. [8] reported the laminar drag reduction of Newtonian fluids in a circular pipe with a highly water-repellent wall, in which the drag reduction ratio was reduced by about 15% in a 12mm-diameter pipe at $Re \leqq 2350$. Furthermore, it has been clarified experimentally that fluid slip occurred at the wall in the laminar flow range. These previously reported experimental and analytical results for flow around a circular cylinder were obtained by applying the no-slip boundary condition at the cylinder wall. Of course, the boundary condition does not contradict these experimental results in general. However, one may be interested as to how the flow patterns change or the value of the drag reduction ratio if the liquid does not stick to the wall. In other words, we can expect to obtain a reduction in the laminar drag of a circular cylinder by using a highly water-repellent coating, because the boundary layer will be laminar in a wide Reynolds number range. In addition, the flow around a circular cylinder is a convenient system for experimentally examining the effect of fluid slip on the flow behavior near the wall because we can easily visualize the flow.

Thus, in this paper, we describe experiments on flow visualization and velocity measurement for a circular cylinder with a highly water-repellent wall in the Reynolds number range of 20 $\sim$150 — a range of some interest in view of the vortex forming that occurs within it. The streamlines of a circular cylinder with fluid slip were obtained by solving the equations of the stream function and the vorticity. The analytical results agree well with the experimental data, which were calculated using the velocity profile of the wake. These results support the qualitative explanation of the reasons for the laminar drag reduction for the drag coefficient of a circular cylinder with a highly water-repellent wall, in which fluid slip occurs.

2. EXPERIMENTAL ARRANGEMENT

The experiments were conducted in a water tunnel with a test section of 400mm×450mm×300 in width, length and depth, respectively. The tunnel was of the closed return type and had a free stream turbulence level of less than 1%. Figure 1 shows the test section of the water tunnel. The test cylinder of 20mm diameter was placed vertically in the test section. Two bronze circular test cylinders, one with a smooth wall and the other with a highly water-repellent wall, were examined to visualize the flow around then and to measure the wake. The circular cylinder with a highly water-repellent wall was coated with poly-tetra-fluoride-ethylene. This is the same coating material as used in the case of the circular pipe to determine laminar drag reduction [8]. Figure 2 shows a micrograph of the surface. It is a smooth surface although it has many fine grooves. The test fluid was tap water at a constant temperature of 14℃. The flow ranges investigated in this study, were the flow patterns of two attached eddies behind the cylinder at Re=20 and 50, and the flow patterns at Re=100 and 150, known as the Kármán vortex street. The velocity profiles of the wake were measured at Re=20 and 50 using a hot-film anemometer at intervals of 1mm across the width of the test section. The Strouhal number was measured using a probe set at a position six times the cylinder radius at Re=100 and 150. The flow patterns around the test cylinder were visualized by a dye streak and a hydrogen bubble method at Re=20, 50, 100 and 150, and photographed using a digital camera. Dye was used as a tracer. Sedimentation did not occur during the measurement. In the hydrogen bubble method, the negative pole wire used was a 50-μm-diameter platinum wire. The effect of the floating velocity of the bubble on the measured value of the separation angle can be neglected because it is 2～4% of the main stream velocity if we calculate it using Stokes' law.

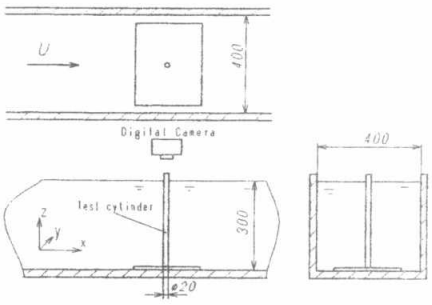

Fig. 1 Test section of water tunnel

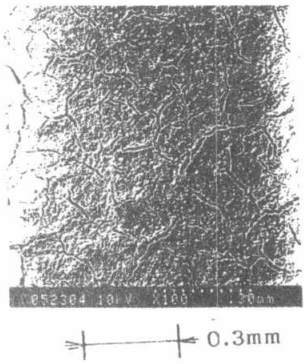

Fig. 2 Micrograph of test highly water-repellent wall

3. EXPERIMENTAL RESULTS AND DISCUSSIONS

3-1 Velocity profile and flow pattern of the wake behind a cylinder

Figure 3 shows the experimental results of the velocity profiles at twice the cylinder radius. In the figure, y and Um are the distance of the span of the test section from the center of the cylinder and uniform velocity, respectively. The width of the wake of the circular cylinder with a highly water-repellent wall is less than that of the smooth circular cylinder at each Reynolds number considered. This means that drag reduction occurs at Re=20 and 50 because the momentum change in the case of the cylinder with a highly water repellent wall is smaller than that of the smooth- wall cylinder. As is well known, two attached eddies are formed behind the cylinder at these Reynolds numbers. Figure 4 shows the nondimensional wake length of the two attached eddies of the flow pattern. Although these eddies enlarge with increase Reynolds number, the value of (s/d) in this experiment at Re≦50 is slightly smaller compared with Son and Hanratty ' data [9]. For the cylinder with a highly water-repellent wall, the value of (s/d) is larger than that of the smooth- wall cylinder. Based on the results of the velocity profile and the wake length, it can be considered that fluid slip occurs at the slender attached eddies of a circular cylinder. With increasing Reynolds

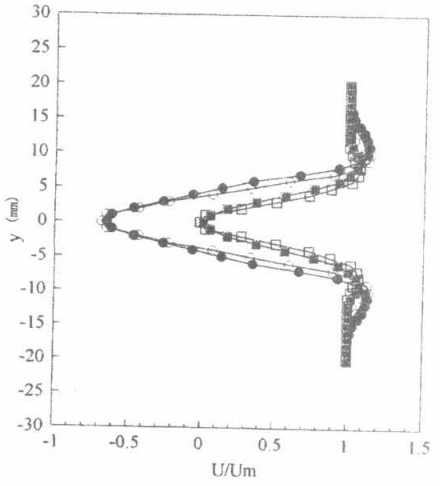

Fig. 3 Velocity profiles of wake of the circular cylinder(x = 2r): ○, Smooth wall, Re=50; □, Smooth wall, Re=20; ●, Highly water-repellent wall, Re=50; ■, Highly water-repellent wall, Re=20

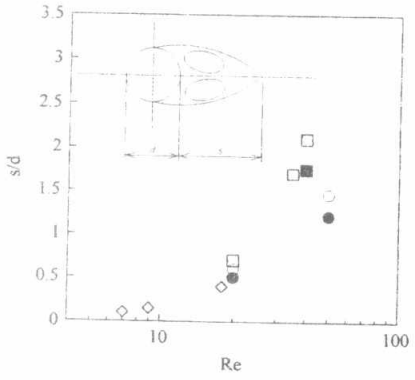

Fig. 4 Relationship between (s/d) and Re: ○, Smooth wall in this study; ●, Highly water-repellent wall in this study; □, Son and Hanratty[9]; ◇, Keller and Takami[10]

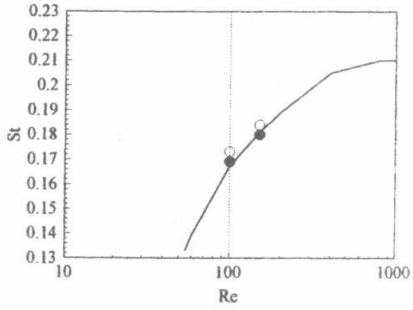

Fig. 5 Strouhal number: Experimental measurements: ●, Smooth wall; ○, Highly water-repellent wall; ——, Roshko[11]

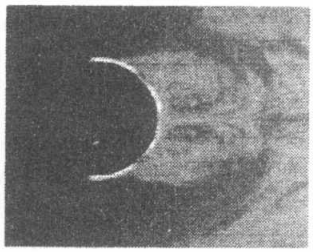

(a) Smooth-wall cylinder

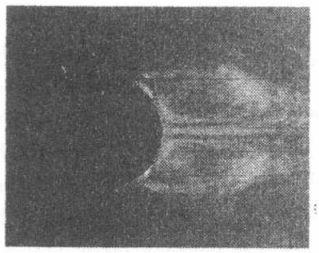

(b) Cylinder with highly water-repellent wall

Fig. 6 Attached eddies on circular cylinders at Re=50

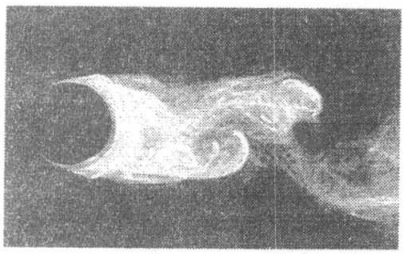

(a) Smooth-wall cylinder

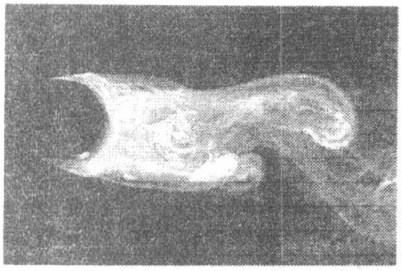

(b) Cylinder with highly water-repellent wall

Fig. 7 Cylinder wakes visualized using dye at Re=150

number a strong regularity in the vorticity of the wake occurs. The Strouhal numbers, St, obtained in this investigation are shown in figure 5. Our experimental data for the smooth-wall cylinder agree with Roshko's data [11], however our data for the cylinder with a highly water-repellent wall have higher values than Roshko's data.

Figures 6(a) ~ (b) and 7(a) ~ (b) show photographs of the flow patterns obtained using a dye feeding method at Re=50 and 150, respectively. In these figures, the top and bottom photographs show the flow patterns for the cylinder with the smooth and the highly water-repellent walls, respectively. The separation point for the flow past a cylinder with a highly water-repellent wall shifts downstream, as shown in figure 6(b), that is, the separation angle is larger than that of the smooth-wall cylinder because the flow velocity of the boundary layer is maintained to some

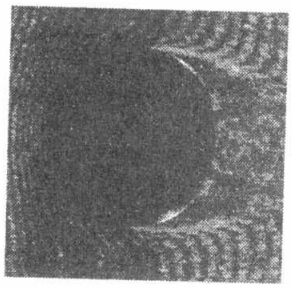

(a) Smooth-wall cylinder

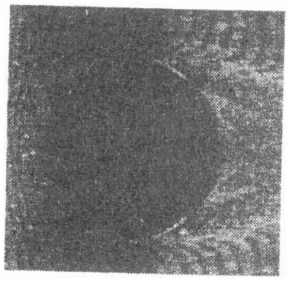

(b) Cylinder with highly water-repellent wall

Fig. 8 Flow past a circular cylinder, visualized using the hydrogen bubble method at Re=50

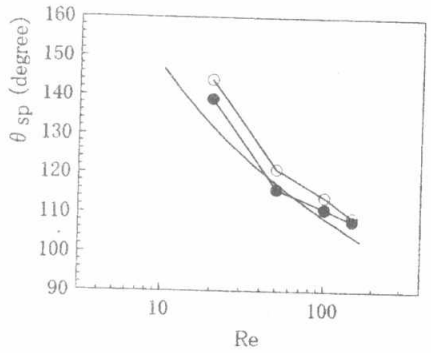

Fig. 9 Variation of the angle of flow separation: ●, Smooth wall in this study; ○, Highly water-repellent wall in this study; —,Pruppacher, et al [2]

degree, by fluid slip at the wall. The shape of the twin attached eddies produced behind the circular cylinder is elongated because of the fluid slip at the wall. In the case of the Kármán vortex street, the starting position also shifts downstream, as shown in figure 7(b).

Because the separation point must be measured accurately to calculate the drag, the hydrogen bubble method was applied for flow visualization. Figure 8 shows an example of a photograph taken with this arrangement. The separation angles measured in this experiment are shown in figure 9, together with other published data [12]. The results for the smooth-wall cylinder agree well with the results reported by other researchers [12]. However, the separation angles of the cylinder with a highly water-repellent wall are larger, compared with the previous data, by about 5～10 degrees. This suggests that drag reduction occurs in it, as stated above.

3-2 Analysis for the flow pattern with fluid slip

In this study, the drag coefficients of a circular cylinder at Re=20 and 50 were obtained were by two methods: (1) by analytical determination from the pressure profile obtained by

numerical calculation, and (2) based on experimental results of the velocity profile for the wake using the momentum equation. For the flow past a circular cylinder in the low-Reynolds- number -range, the streamlines can be determined by solving the equations for the stream-function and the vorticity using the numerical calculation model. For an incompressible fluid, the equations for the stream function, ϕ, and the vorticity, ω, which are written using the polar coordinates, are given as follows,

$$\frac{\partial^2 \phi}{\partial \xi^2} + \frac{\partial^2 \phi}{\partial \theta^2} = -\omega e^{2\xi} \tag{1}$$

$$\frac{\partial \omega}{\partial t} + e^{-2\xi}\left(\frac{\partial \phi}{\partial \xi}\frac{\partial \omega}{\partial \theta} - \frac{\partial \phi}{\partial \theta}\frac{\partial \omega}{\partial \xi}\right) = \frac{e^{-2\xi}}{\mathrm{Re}}\left(\frac{\partial^2 \omega}{\partial \xi^2} + \frac{\partial^2 \omega}{\partial \theta^2}\right) \tag{2}$$

The boundary conditions of the stream function at the cylinder wall and in the free-stream region are

$r = a$ $\qquad \phi_a = 0$ (3)

$r \to \infty$ $\qquad \phi_\infty = y = e^{\xi} \sin\theta$ (4)

For the vorticity, the boundary conditions are given as follows,

$r = a$ $\qquad \omega_0 = -e^{-2\xi}\, \partial^2 \phi / \partial \xi^2$ (5)

$r \to \infty$ $\qquad \omega_\infty = 0$ (6)

From the finite-difference approximation of equation (5), we obtain the following equation by applying $\xi = 0$ and $\phi = 0$ at the cylinder wall,

$$\omega_o = -(\phi_{k+1} + \phi_{k-1})/(\Delta\xi)^2 \tag{7}$$

where, ϕ_{k+1} and ϕ_{k-1} are the grid points. The slip velocity at the cylinder wall is given as,

$$v_\theta = (\phi_{k+1} - \phi_{k-1})/\Delta\xi = u_s \tag{8}$$

where, us is the slip velocity.
By combining equations (7) and (8), we get

$$\omega_o = (u_s\Delta\xi - 2\phi_{k+1})/(\Delta\xi)^2 \tag{9}$$

The initial conditions are

$$\phi = (r - (\frac{1}{r}))\sin\theta = (e^{\xi} - e^{-\xi})\sin\theta \tag{10}$$
$$\omega = 0$$

By applying these boundary conditions, equations (1) and (2) are solved using a finite-difference model in for numerical methods. For the model, we used the polar coordinates 60×40 mesh. The slip velocity at the wall, which must be given in the calculation, and is calculated using the following equation obtained by Navier [13]. It has also been examined for flow in a circular pipe [8] and between two coaxial rotating cylinders by Watanabe and Akino [14] at a highly water-repellent wall. The shear stress, τ_w is expressed as

$$\tau_w = \mu \left| \frac{\partial u}{\partial y} \right|_{y=0} = \beta u_s \tag{11}$$

where μ, u_s and β are respectively, the viscosity, the slip velocity at the wall and the sliding coefficient, which is related to the viscosity μ and the characteristics of the wall surface, respectively. Equation 11 reduces to the no-slip boundary condition if β equals infinity. Although we can measure the value of the sliding coefficient for each flow field, it generally cannot be accurately established because it depends on the viscosity and the characteristics of the wall surface. After assuming a value of the sliding coefficient β, the slip velocity was determined in the numerical calculation step using equation 7. Figure 10 shows an example of the slip velocity calculated in this manner. At present, we cannot determined the value of β for this flow field, as described above. Thus, we solved these equations for the three cases of β=10, 4 and 2 (Pa · s/m). Figures 11(a) ~ (d) show the streamlines of the numerical solutions for the flow past a circular cylinder at Re=50 for these cases. Figure 11(a) shows the streamlines in the case of the no-slip condition, where the standing eddies, whose size increases with Reynolds number, have formed behind the circular cylinder. The calculated

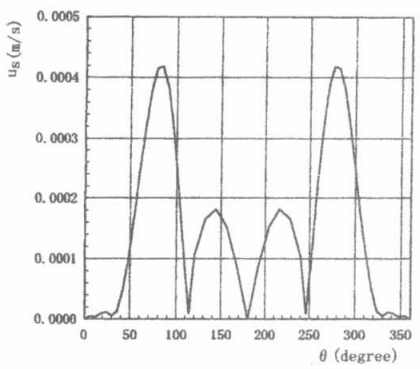

Fig. 10 Calculated slip velocity(β =4Pa·s/m)

result agrees well with the experimental result of the flow pattern shown in figure 5. In the case of fluid slip, the results indicate that the standing eddies elongate downstream for β less than 4 (Pa·s/m). This phenomenon coincides with the decrease of the width of the wake shown in figure 3. With the increase of β, the size of the eddies decreases, as shown in figure 11(d). This means that the flow pattern approaches that of an ideal fluid with the increase of slip velocity. Consequently, the flow pattern in the case of β =4 (Pa·s/m) agrees with the experimental result. The value of β agrees with the value assumed for the flow in a pipe [8] and the enclosed rotating disk [15] with a highly water-repellent wall.

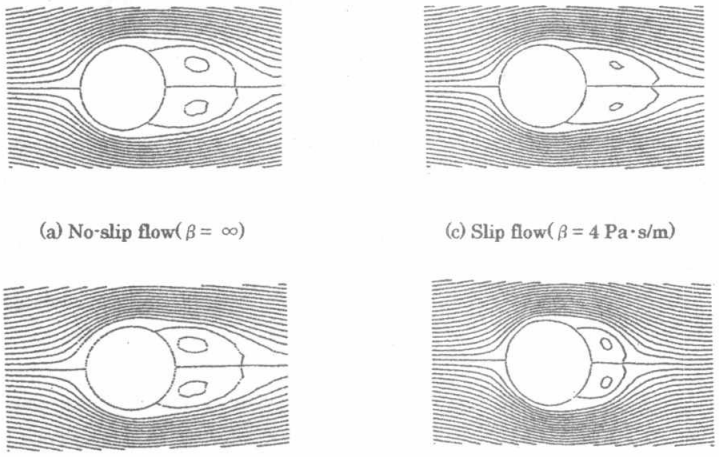

(a) No-slip flow($\beta = \infty$)

(c) Slip flow(β = 4 Pa·s/m)

(b) Slip flow(β = 10 Pa·s/m)

(d) Slip flow(β = 2 Pa·s/m)

Fig.11 Streamlines around circular cylinders at Re = 50

3-3 Measurement of drag coefficient

If we neglect friction drag for the total drag of a circular cylinder, the drag coefficient, Cd, can be calculated as

$$Cd = \int_0^{2\pi} 2\,(P - P_\infty)/\rho\,Um^2\,\cos\theta\,d\theta \qquad (12)$$

where p is the calculated pressure profile of the circular cylinder. ρ, p_∞ and U_m are the density, the pressure and the velocity of the uniform flow, respectively. We calculated the pressure profile for the case of β=4 (Pa·s/m). Figure 12 shows the drag coefficient calculated using equation (12). Roshko's data [3] are represented by the solid line in the figure for comparison with values for the smooth-wall cylinder. Although the value of the drag coefficient at Re=10 under the no-slip condition is below the solid line, the data for Re=50 approach it. The value of the drag coefficient for the circular cylinder with fluid slip, the sliding coefficient of which equals β=4 (Pa·s/m), is smaller than that under the no-slip condition, that is, drag reduction is included in it. The drag reduction ratios at Re=10 and 50 are about 15% and 10%, respectively.

We also calculated the drag for the test cylinder with a highly water-repellent wall using the value of the velocity profile of the wake.

The drag D, is given as

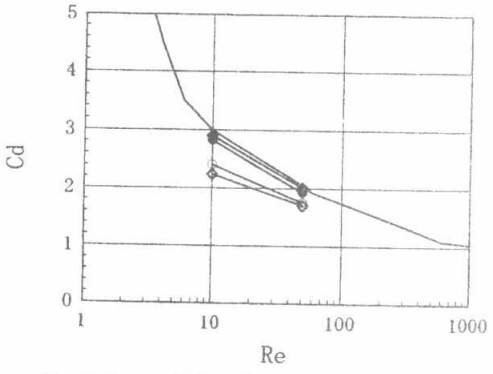

Fig. 12 Drag coefficient, Experimental values obtained from wake velocity profile: ◆, Smooth wall; ◇, Highly water-repellent wall, Calculated data obtained from pressure profile: ●, Smooth wall; ○, Highly water-repellent wall; ——, Roshko[3]

$$D = \rho L \int_{-\infty}^{\infty} Um\,(Um - U)\,dy \qquad (13)$$

where, ρ and L are the density and length of the cylinder, respectively. Um and U are the uniform flow and wake velocities, respectively. The results calculated using equation (13) are shown in figure 12. The data agree well with the result calculated from the pressure profile at Re=50, although the difference is slight at Re=20. On examining these results

and figure 12, two trends become apparent for drag reduction: (1) the agreement between the calculation and the experiment is good at Re=50, and (2) the drag reduction ratio decreases with the increase of the Reynolds number. The drag coefficient obtained experimentally is slightly larger than the calculated drag coefficient. To quantify these results, the determination of the sliding coefficient, β, is required.

4. CONCLUDING REMARKS

By measuring the velocity of the wake behind a circular cylinder with a highly water-repellent wall, it was demonstrated that drag reduction occurs at Re=10 and 50, at drag reduction ratios of about 25 % and 15% , respectively. The results indicate that the separation point shifts downstream because of fluid slip at the cylinder wall. These phenomena were examined by flow visualization of the flow pattern around the circular cylinder. With the streamlines calculated by applying the boundary condition of the slip velocity at the wall, the flow patterns were in good agreement with the experimentally obtained traces. The calculated drag coefficients of Re = 10 and 50 have 15% and 10% drag reduction ratios, respectively if we assume the sliding coefficient, β to be 4 (Pa·s/m). These values are slightly smaller than the experimental values obtained from the wake velocity profile. However, the problem of determining the value of the sliding coefficient remains, although Navier's equation for fluid slip is applicable under the present boundary conditions for the analysis of fluid slip at the wall.

We thank E. Nakatani, Y. Doi and N. Harutani of Kansai Paint Co., Ltd., for their support in setting up the experimental apparatus. This work was supported financially by the Scientific Research Fund of the Ministry of Education, Science, Sports and Culture of Japan (B-09450082).

REFERENCES

[1] Finn, R. K., 1953 Determination of the drag on a cylinder at low Reynolds numbers. J. Applied Physics, vol. 24, no. 6, pp.771-773.

[2] Pruppacher, H.R., Clair, B. P. L. and Hamielec, A. E. 1970 Some relations between drag and flow pattern of viscous flow past a sphere and a cylinder at low and intermediate Reynolds numbers. J. Fluid Mech., vol. 44, part 4, pp.781-790.

[3] Roshko, A. 1960 Experiments on the flow past a circular cylinder at very high Reynolds number. J. of Fluid Mech., vol. 10, pp. 345-356.

[4] Tritton, D.J., 1959 Experiments on the flow past a circular cylinder at low Reynolds

numbers. J. of Fluid Mech., vol. 6, pp. 547-567.

[5] Wieselsberger, C. 1921 Neuere Feststelleungen über die Gesetze des Flüssigkeits- und Luftwiderstands. Phys.Z. 22, pp. 321-328.

[6] Toms, A.B., 1949 Some Observations on the Flow of Linear Polymer Solutions Through Straight Tubes at Large Reynolds Numbers. Proc. Inter. Cong. On Rheology, Vol. II ,pp.135.

[7] Hoyt, J.W., 1972 The Effect of additives on Fluid Friction The transaction of the ASME, Ser.D, pp. 258-285.

[8] Watanabe, K., Yanuar and Udagawa, H. 1999 Drag reduction of Newtonian fluid in a circular pipe with a highly water-repellent wall. vol. J. Fluid Mech. vol.381, pp. 225-238.

[9] Son, J. S. and Hanratty, T. J. 1969 Numerical solution for the flow around a cylinder at Reynolds numbers of 40, 200 and 500. J. Fluid Mech. vol.35, part 2, pp.369-386.

[10] Keller, H. B. and Takami, H., 1966 Numerical Solutions of Non-Linear Differential Equations Proc. of Adv. Symp. pp.115-121.

[11] Roshko, A., 1953 Development of Turbulent wakes from Vortex streets, NACA TN. 2913.

[12] Hamielec, A. E., Storey, S. H. and Whitehead, J. M., 1962 Viscous Flow Around Fluid Spheres at Intermediate Reynolds Number(II). Can. J. Chem. Engng., 41, pp246-251.

[13] Navier, C.L.M.H. 1823 Memories de l' Academie Royale des Sciences de l'Institute de France, 1, pp. 414-416.

[14] Watanabe, K. and Akino, T. 1999 Drag Reduction in Laminar Flow Between Two Vertical Coaxial Cylinders, Trans. of the ASME, J. Fluids Eng, vol. 121, pp. 1-7. (in printing)

[15] Watanabe, K. and Ogata, S 1997 Drag Reduction for a Rotating Disk with Slip in Newtonian Fluids, Proc. of Inter. Conf. On Fluid Engineering, pp. 545-550.